

Electronic Supplementary Information for

Advanced emulsions via noncovalent interaction-mediated interfacial self-assembly

Songling Han, Huijie An, Hui Tao, Lanlan Li, Yuantong Qi, Yongchang Ma, Xiaohui Li, Ruibing Wang*,
and Jianxiang Zhang*

*Corresponding authors:

Ruibing Wang, PhD, Prof.

Email: rwang@umac.mo

Jianxiang Zhang, PhD, Prof.

Email: jxzhang1980@gmail.com

Department of Pharmaceutics

College of Pharmacy

Third Military Medical University

Materials and Methods

Chemicals

L-Aspartic acid β -benzyl ester was purchased from Chem-Impex International, Inc (USA). Triphosgene was obtained from TCI Chemicals (Japan). α -Methoxy- ω -amino-polyethylene glycol (PEG-NH₂) with average molecular weight (M_w) of 5 or 2 kDa was purchased from Laysan Bio, Inc (Alabama, USA). Ethylenediamine (EDA), diethylenetriamine (DETA), triethylenetetramine (TETA), *n*-valeric acid (VAL), *n*-hexanoic acid (HEX), and *n*-heptanoic acid (HEP) were obtained from Aladdin Reagent Co., Ltd. (China). Nile red and pyrene were obtained from J&K Scientific Ltd. Poly(lactide-*co*-glycolide) (PLGA, 50:50, with intrinsic viscosity of 0.6 dl g⁻¹) was purchased from PolySciTech (USA). Au or Ag nanocrystal powders were obtained from Ocean NanoTech, LLC (USA). Polyethylene glycol-*block*-poly(N-isopropylacrylamide) (PEG-PNIPAm, M_w of PEG 5 kDa, while M_w of PNIPAm was 22 kDa) was purchased from Polymer Source (Canada). All the other reagents are commercially available and used as received.

Synthesis of polyethylene glycol-*block*-poly(β -benzyl L-aspartate) (PEG-PBLA)

β -Benzyl L-aspartate N-carboxyanhydride (BLA-NCA) was synthesized according to literature.¹ Specifically, 10 g L-aspartic acid β -benzyl ester was suspended in 100 ml anhydrous THF, and then 6.3 g triphosgene in 80 ml THF was added. This reaction mixture was stirred magnetically for 2 h at 40°C under nitrogen atmosphere. Thus obtained transparent solution was concentrated under a reduced pressure and the obtained white oil was recrystallized three times from a mixture of THF/petroleum ether, and finally dried at room temperature under vacuum. Subsequently, PEG-PBLA was synthesized by PEG-NH₂ initiated polymerization of BLA-NCA in DMF at 40°C.¹

Synthesis of cationic diblock copolymers with different amine groups

A modified quantitative aminolysis reaction was employed to prepare different cationic diblock copolymers derived from PEG-PBLA.² Briefly, 1.0 g PEG-PBLA was dissolved in dry DMSO at 40°C, into which a 50-fold molar excess of EDA, DETA, or TETA was added. After 48 h of reaction, the solution was dialyzed against deionized water. The final copolymers PEG-PEDA, PEG-PDETA, or PEG-PTETA were separately obtained by lyophilization.

Measurements

¹H NMR and ¹H-¹H COSY spectra were recorded on an Agilent 600 MHz spectrometer. Fourier transform infrared (FT-IR) spectra were acquired on a Perkin-Elmer FT-IR spectrometer (100S). Dynamic light scattering and ξ -potential measurements were performed on a Malvern Zetasizer Nano ZS instrument. The freshly prepared solution samples were diluted according to their scattering intensities for size determination. Unless stated otherwise, measurements were implemented at 25°C. Transmission electron microscopy (TEM) observation was carried out on a JEM-1400 microscope (JEOL, Japan) operating at an acceleration voltage of 100 kV. Confocal laser scanning microscopy (CLSM) was performed on a Carl ZEISS LSM780 NLO fluorescence microscope, while super-resolution fluorescence microscopy (SRFM) was carried on a DeltaVision OMX Blaze microscope (GE Healthcare, USA). Matrix-assisted laser desorption/ionization time-of-flight (MALDI-TOF) mass spectrometry was carried on a MALDI-7090 instrument (Shimadzu, Japan). Viscosity was recorded on a Discovery HR-1 rheometer (TA Instruments, USA).

Fabrication of emulsions based on hydrophilic diblock copolymers and various oil molecules

As a general procedure, emulsions were formed by adding various volumes of oil-phase molecules in 1 ml of aqueous solutions containing diblock cationic copolymers at different concentrations, which was followed by vortexing for 30 s. For catastrophic phase inversion studies, after the oil phase was added into the aqueous phase, the mixture was gently shaken to give rise to emulsions with relatively large sizes.

Preparation of complex emulsions

To prepare water-in-oil-in-water (w/o/w) complex emulsions, primary w/o emulsion was first obtained by emulsifying inner aqueous solution containing PEG-PEDA into the oil phase of HEX by vortexing for 30 s. Thus obtained w/o emulsion was emulsified with an outer water phase containing PEG-PEDA by gently shaking. The similar procedures were followed to fabricate oil-in-water-in-oil (o/w/o) complex emulsions. In both cases, the oil phase was doped with Nile red for observation by fluorescence microscopy. Of note, morphology of complex emulsions can be regulated by adjusting the volume ratios of different phases.

Isothermal titration calorimetry

Isothermal titration calorimetry (ITC) experiments were performed using a MicroCal iTC200 Microcalorimeter (GE Healthcare, USA) at 25°C. The reference cell was filled with distilled water. An initial 0.4 μ l injection was discarded from each data set in order to remove the effect of titrant diffusion across the syringe tip during the equilibration process. The experiment consisted of injecting 2 μ l (19 injections, 0.4 μ l for the first injection only) of various aliphatic acids at a concentration of 1 mM into the reaction cell initially containing 200 μ l of PEG-PEDA solution at 0.02 mM. A background titration was performed using an identical titrant with distilled water placed in the sample cell. The result was subtracted from each experimental titration to account for the heat of dilution. The titrant was injected at 2 min intervals to ensure that the titration peak returned to the baseline prior to the next injection. Each injection lasted 4 s. To ensure a homogeneous mixing in the cell, the stirring speed was kept constant at 1000 rpm. Results of the titration curves were analyzed using Origin software supplied by MicroCal under a single binding site model.

Fluorescence spectroscopy measurement of different systems

Sample solutions for fluorescence measurements were prepared as described previously.³ Briefly, pyrene in acetone was added to each of a series of 2 ml vials, and acetone was evaporated. A total of 1 ml of various concentrations of HEX/PEG-PEDA at various oil-water ratios was added to each vial and heated at 50°C for 10 h, and then left to cool for 10 h at room temperature. The final concentration of pyrene was 6.0×10^{-7} M. Steady-state fluorescent spectra were acquired using a F-7000 fluorescence spectrophotometer (Hitachi, Japan) with a slit width of 2.5 nm for both excitation and emission. All spectra were run on air-equilibrated solutions. For fluorescence excitation spectra, the emission wavelength was 390 nm, with scan speed of 240 nm min⁻¹. All the experiments were carried out at 25°C.

Interfacial tension measurements

The maximum bubble pressure method was used to measure interfacial tension of different oil-water systems, using a surface tension measuring instrument (Model DP-AW-II, Sangli, China). Specifically, the

tip of a capillary tube was adjusted to ensure it is immersed in the oil/water interface. The gas flow into the device creates bubbles at a capillary orifice at a constant and controlled frequency. These bubbles grow with increasing in the internal pressure, due to the energy cost upon generation of the bubble surface. The pressure inside the bubble was monitored and the maximum value was identified, corresponding to the point when the bubble reached a hemispherical shape. The resulting maximum pressure drop ΔP_{\max} across the bubble surface was then substituted into the Young-Laplace equation to determine the surface tension σ based on the equation

$$\sigma = \frac{r}{2} \Delta P_{\max} = K \Delta P_{\max}$$

where r is the radius of the surface curvature. For a bubble with a hemispherical shape, r is equal to that of the capillary orifice. K is a constant calculated using distilled water under the same experimental conditions.

Viscosity measurement

A TA Discovery HR-1 rheometer (TA Instruments, USA) was used, which is equipped with a 40-mm plate geometry on a smooth aluminium Peltier-thermostated surface (25°C). A velocity of 18.84 rad s⁻¹ was used for the peak hold experiments in a flow mode, which was verified for measuring viscosity of different aqueous solutions.

Calculation of hydrophilic-lipophilic balance (HLB) values

HLB values of different aliphatic acids and cationic copolymers were calculated according to the group contribution method established by Davies.⁴ Specifically, the HLB value is given by

$$\text{HLB} = 7 + \sum(\text{hydrophilic group numbers}) + \sum(\text{lipophilic group numbers})$$

Fabrication of polymeric nanoparticles based on assembled emulsions

To prepare polymer nanoparticles using HEX/PEG-PEDA nanoemulsions, 100 μl dichloromethane containing 5 mg PLGA was added into 1 ml nanoemulsions formed by 1 ml aqueous solution of PEG-PEDA (10 mg ml⁻¹) and 10 μl HEX. After further emulsification, the obtained emulsions were stirred at room temperature for 4 h. The solidified polymeric nanoparticles were collected by centrifugation and washed with deionized water for additional characterization.

Statistical analysis

Statistical analysis was performed by SPSS 19.0 using one-way ANOVA test for experiments consisting of more than two groups, and with a two-tailed, unpaired t -test in experiments with two groups. Statistical significance was assessed at $p < 0.05$.

References

- (1) Zhang, J. X.; Ma, P. X. *Polymer* **2011**, 52, 4928-4937.
- (2) Miyata, K.; Oba, M.; Nakanishi, M.; Fukushima, S.; Yamasaki, Y.; Koyama, H.; Nishiyama, N.; Kataoka, K. *J. Am. Chem. Soc.* **2008**, 130, 16287-16294.
- (3) Wilhelm, M.; Zhao, C. L.; Wang, Y.; Xu, R.; Winnik, M. A.; Mura, J. L.; Riess, G.; Croucher, M. D. *Macromolecules* **1991**, 24, 1033-1040.
- (4) Davies, J. T. In *Proceedings of 2nd International Congress Surface Activity* London, 1957, p 426-438.

Table S1. Physicochemical properties of different cationic PEG copolymers.

| Copolymers | PEG block | Polyaspartamide | Length of polyaspartamide block | Calculated HLB |
|--------------------------|------------------|------------------------|--|-----------------------|
| PEG-PEDA | 5 kDa | PEDA | 22 | 209 |
| PEG-PDETA | 5 kDa | PDETA | 19 | 168 |
| PEG-PTETA | 5 kDa | PTETA | 16 | 133 |
| PEG _{2k} -PEDA | 2 kDa | PEDA | 24 | 201 |
| PEG _{2k} -PDETA | 2 kDa | PDETA | 15 | 119 |
| PEG _{2k} -PTETA | 2 kDa | PTETA | 17 | 116 |

Table S2. Physicochemical properties of PEG-PNIPAm.

| Copolymer | PEG block | PNIPAm block | Length of PNIPAm block | Calculated HLB |
|------------------|------------------|---------------------|-------------------------------|-----------------------|
| PEG-PNIPAm | 5 kDa | 22 kDa | 195 | 49 |

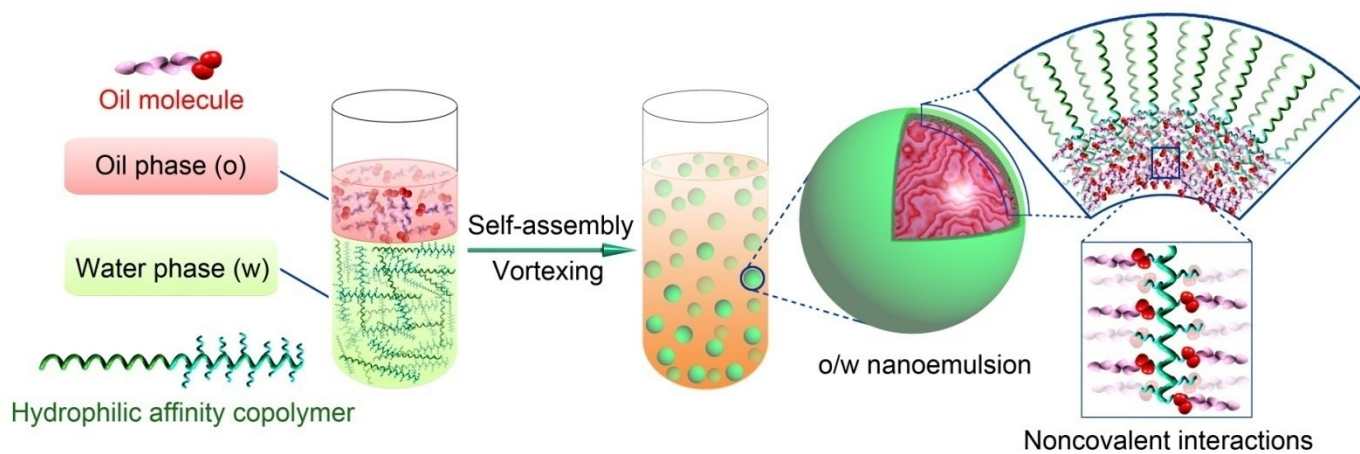


Figure S1. Schematic illustration of emulsification by non-covalent interaction-mediated self-assembly of affinity copolymers at the oil-water interface.

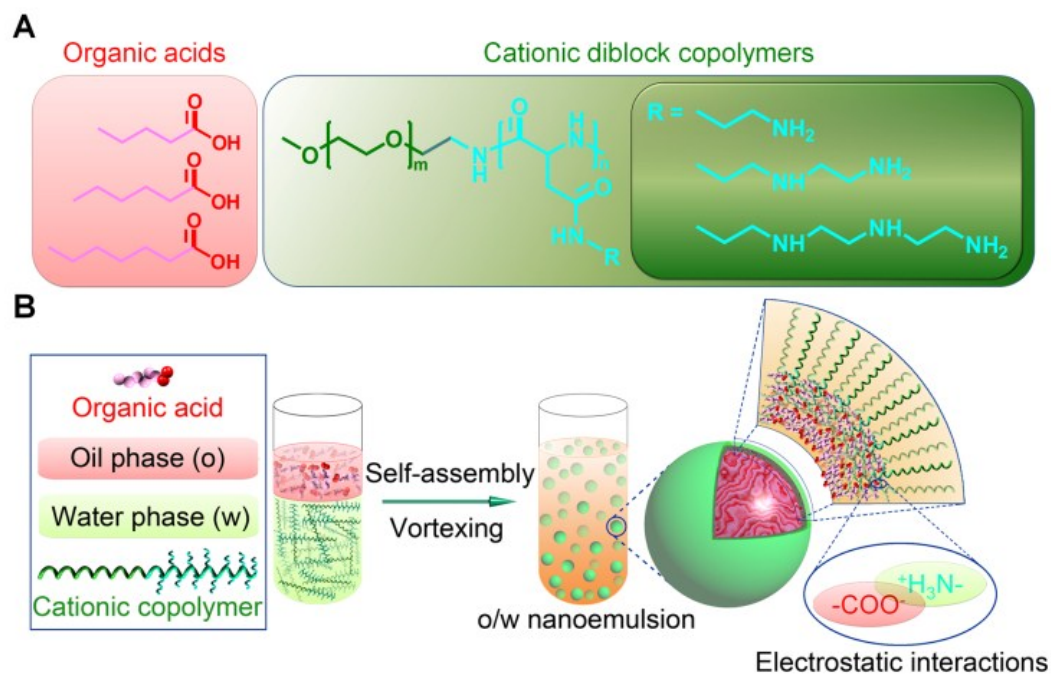


Figure S2. Self-assembling emulsions. (A) The chemical structures of oil phase molecules and hydrophilic copolymers used for the preparation of emulsions. (B) Schematic of self-assembly emulsions by electrostatic force-mediated assembly of cationic diblock copolymers at the oil-water interface.

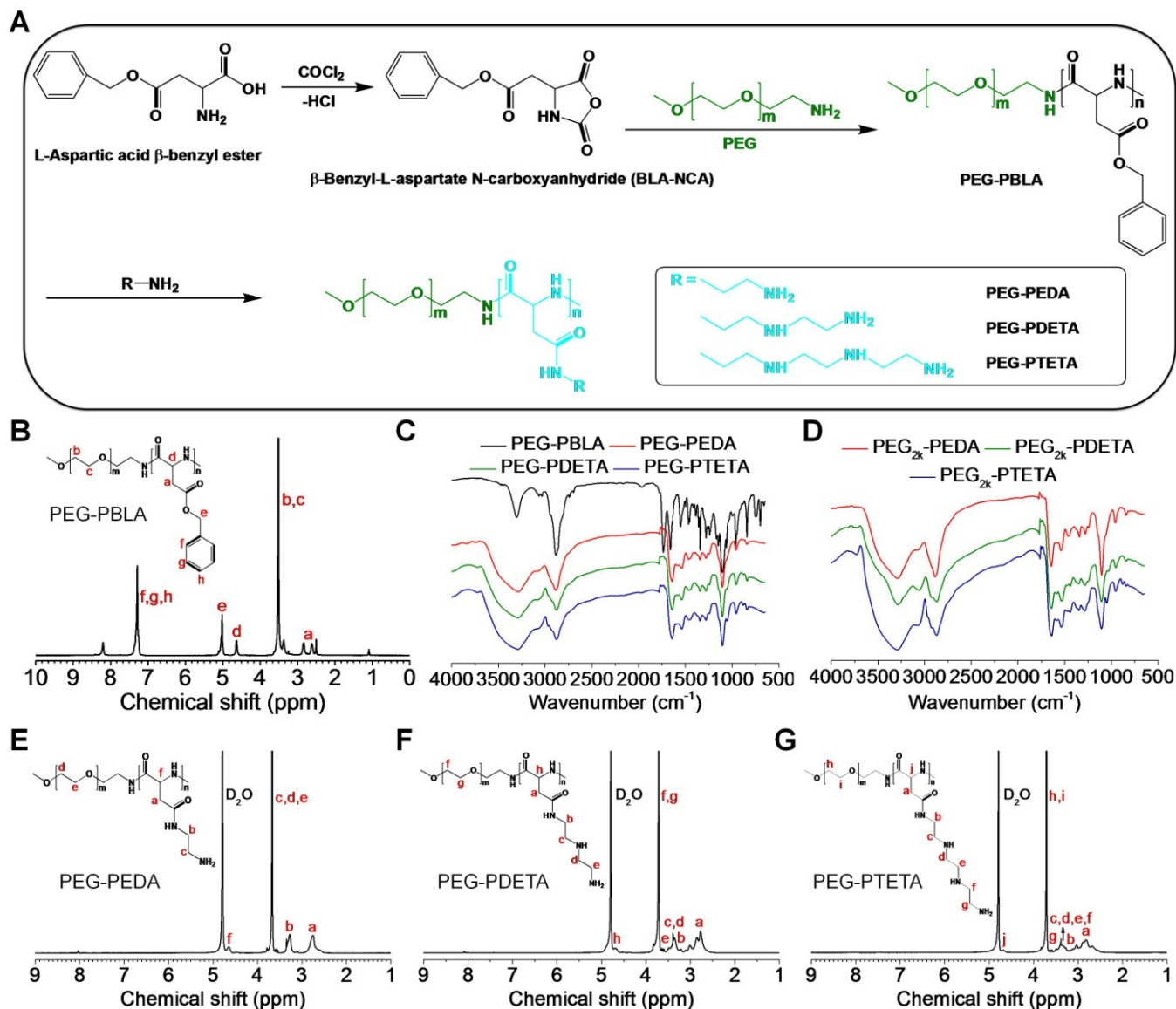


Figure S3. Synthesis of different cationic diblock copolymers with one PEG block and another polyaspartamide block. (A) Schematic illustration of the synthetic route. (B) ¹H NMR spectrum of polyethylene glycol-*block*-poly(β -benzyl L-aspartate) (PEG-PBLA). The molecular weight of PEG is 5 kDa, while the block length of PBLA is about 20. (C) FT-IR spectra of PEG-PBLA and the corresponding polyaspartamide copolymers including PEG-PEDA, PEG-PDETA, and PEG-PTETA. PEG-PEDA, PEG-PDETA, and PEG-PTETA were derived by aminolysis of PEG-PBLA with ethylenediamine (EDA), diethylenetriamine (DETA), and triethylenetetramine (TETA), respectively. Unless otherwise stated, M_w of PEG was 5 kDa in PEG-PBLA and corresponding cationic copolymers. (D) FT-IR spectra of cationic diblock copolymers PEG_{2k}-PEDA, PEG_{2k}-PDETA, and PEG_{2k}-PTETA derived from of PEG_{2k}-PBLA with a PEG block of 2 kDa. (E-G) ¹H NMR spectra of cationic diblock copolymers PEG-PEDA (E), PEG-PDETA (F), and PEG-PTETA (G).

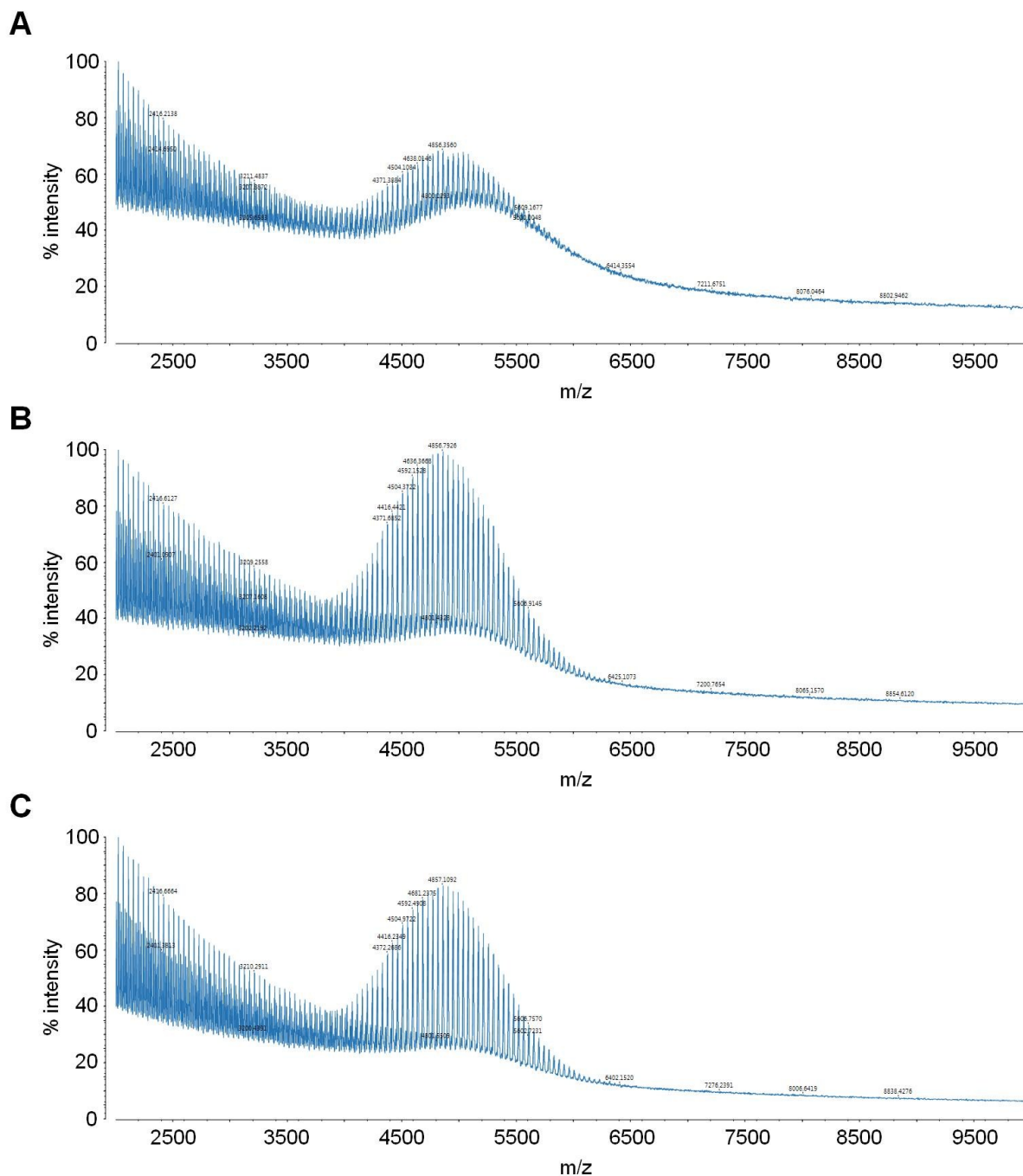


Figure S4. Characterization of different copolymers by matrix-assisted laser desorption ionization time-of-flight (MALDI-TOF) mass spectrometry. (A-C) MALDI-TOF mass spectra of PEG-PEDA (A), PEG-PDETA (B), and PEG-PTETA (C).

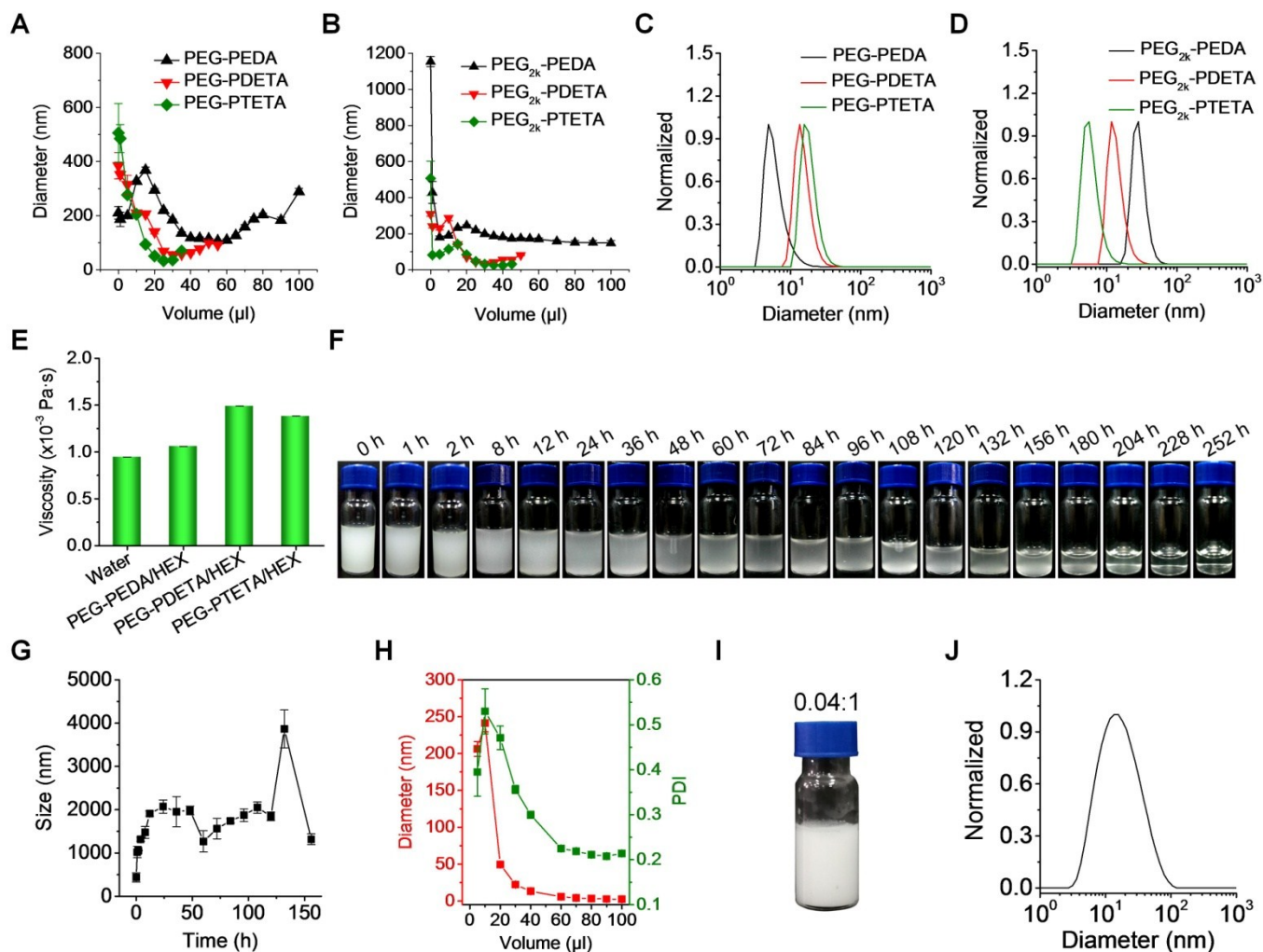


Figure S5. Electrostatic force-mediated assembly of emulsions by aliphatic acids and cationic copolymers. (A-B) The average diameter of aqueous solutions of cationic copolymers with a PEG block of 5 kDa (A) or 2 kDa (B) and different polyaspartamide blocks upon addition of increased volumes of HEX in 1 ml of aqueous solution containing 10 mg ml⁻¹ copolymers. (C-D) Size distribution profiles of emulsions formed by HEX and aqueous solutions of cationic copolymers with a PEG block of 5 kDa (C) or 2 kDa (D) and different polyaspartamide blocks at the oil-water volume ratio of 0.04:1. The copolymer concentration was 10 mg ml⁻¹. (E) Viscosity values of different solutions. For different copolymers, their concentration in deionized water was 10 mg ml⁻¹. (F-G) Digital photos (F) and quantified mean diameter (G) of VAL/PEG-PEDA w/o nanoemulsions during long-term incubation at room temperature. The oil-water volume ratio was 0.05:1. After 120 h, a clear phase separation was observed. (H) The average diameter and PDI values of 1 ml of aqueous solution containing 10 mg ml⁻¹ PEG-PEDA upon addition of increased volumes of oleic acid. (I-J) A typical digital photo (I) and size distribution (J) of oleic acid/PEG-PEDA assembled nanoemulsions. The concentration of PEG-PEDA was 10 mg ml⁻¹, while the volume ratio of oleic acid to aqueous solution of PEG-PEDA was 0.04:1. Data in (A, B, E, G, H) are mean \pm s.d. ($n = 3$).

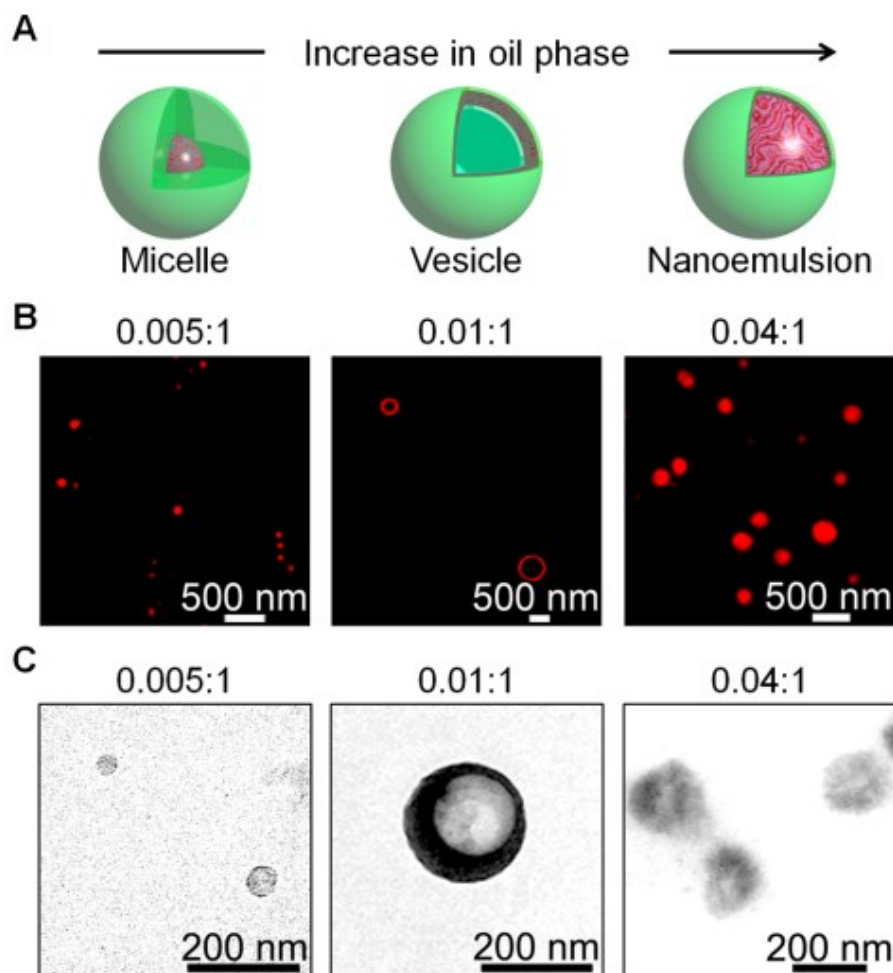


Figure S6. The aliphatic acid content-dependent structural transition. (A-C) Schematic (A) as well as SRFM (B) and TEM (C) images indicating transition from micelles, vesicles, to nanoemulsions of HEX/PEG-PEDA with the increased oil-water ratio.

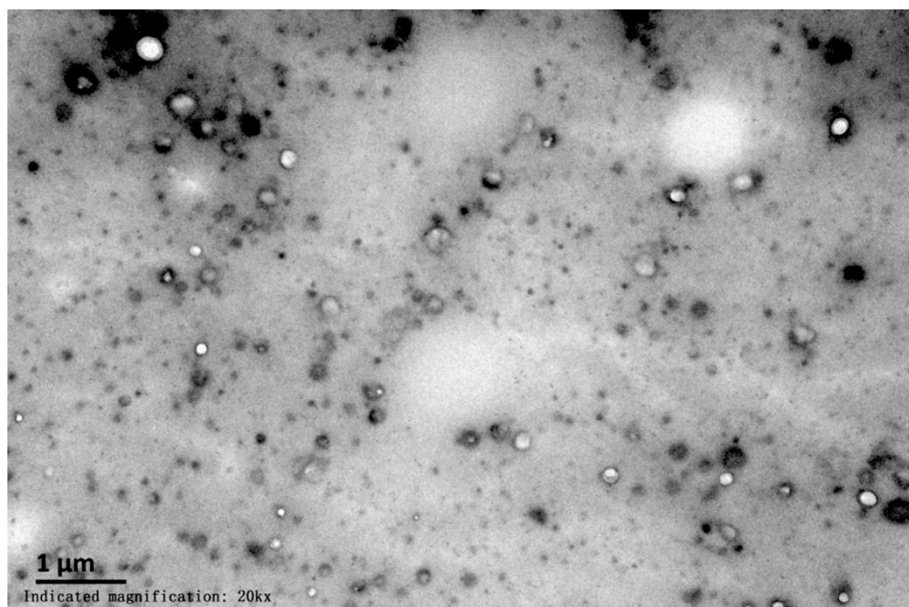


Figure S7. A representative low resolution TEM image of HEX/PEG-PEDA assembled vesicles. The PEG-PEDA concentration was 10 mg ml^{-1} , while the volume ratio of HEX to aqueous solution of PEG-PEDA was 0.01:1.

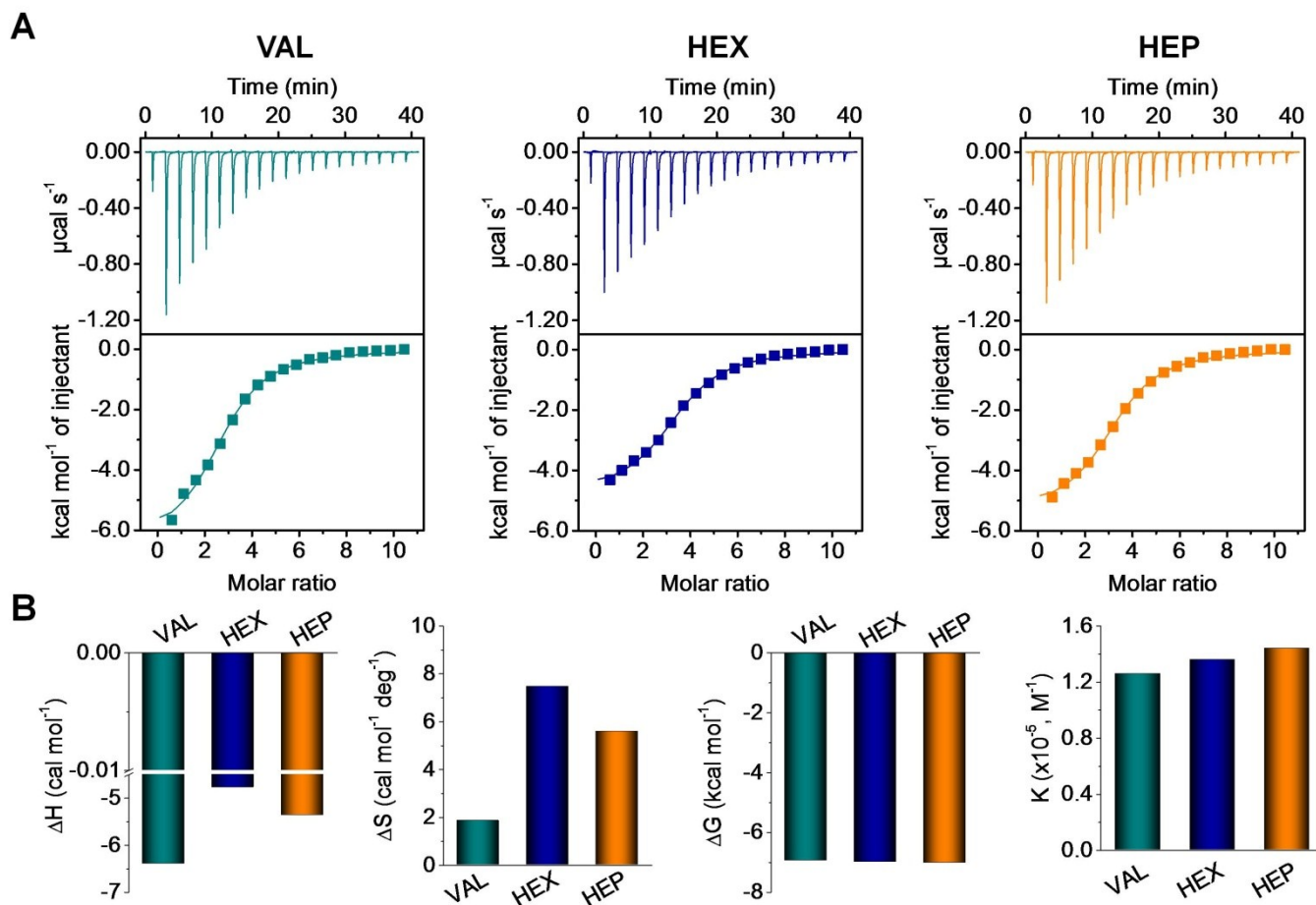


Figure S8. Characterization of interactions between PEG-PEDA and hydrophobic aliphatic acids by isothermal titration calorimetry (ITC). (A-B) ITC curves (A) and calculated thermodynamic parameters and binding constants (B) between PEG-PEDA and different aliphatic acids of *n*-valeric acid (VAL), *n*-hexanoic acid (HEX), and *n*-heptanoic acid (HEP). ΔH , the change in enthalpy; ΔS , the change in entropy; ΔG , the change in Gibbs free energy; and K , the binding constant. The concentration of aliphatic acids was 1 mM, while it was 20 μ M for PEG-PEDA in all cases.

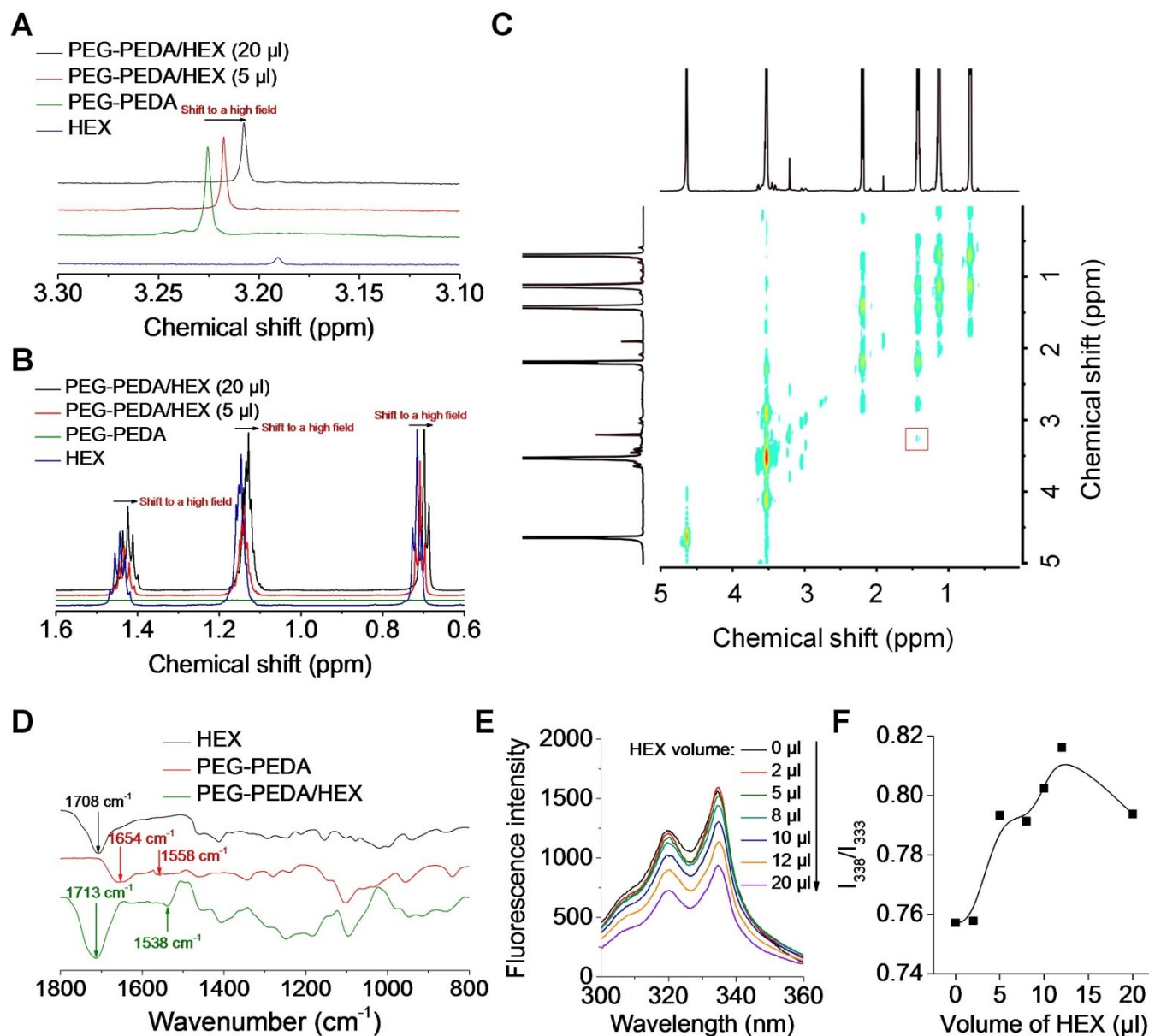


Figure S9. Characterization of interactions between PEG-PEDA and hydrophobic aliphatic acids by different spectrometric techniques. (A-B) Changes in ^1H NMR spectra of PEG-PEDA/HEX in D_2O with increased contents of HEX. In this case, 10 mg copolymer was dissolved in 1 ml of D_2O . (C) The ^1H - ^1H COSY spectrum of PEG-PEDA and HEX. ^1H - ^1H COSY NMR spectroscopy indicated correlation signals between HEX and EDA moieties of PEG-PEDA. (D) FT-IR spectra of HEX, PEG-PEDA, and PEG-PEDA/HEX mixture. (E) Excitation fluorescence spectra of pyrene in aqueous solution of PEG-PEDA with increased HEX. (F) The plot of intensity ratios at 338 and 333 nm from excitation spectra.

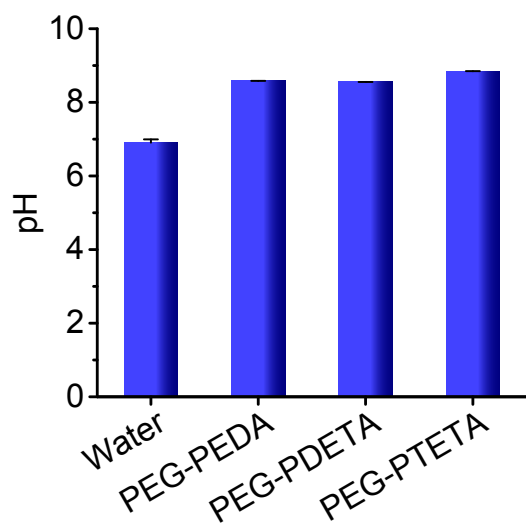


Figure S10. The quantified pH values of different aqueous solutions. For all solutions containing copolymers, their concentration was 10 mg mL⁻¹. Data are mean ± s.d. ($n = 3$).

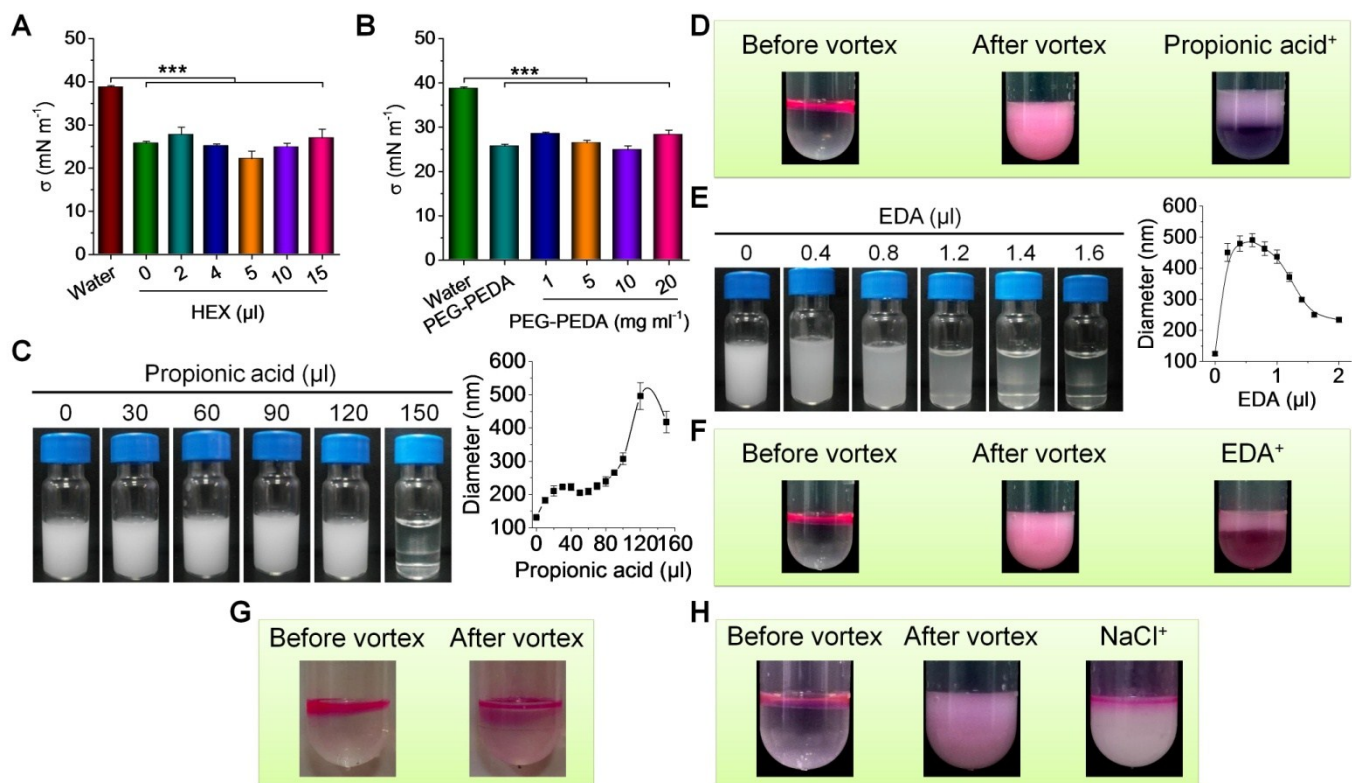


Figure S11. Chemical-induced emulsion breaking of assembled HEX/PEG-PEDA o/w nanoemulsions. (A) Interfacial tension of HEX and deionized water in the absence or presence of PEG-PEDA pre-incubated with HEX. In all cases, 1 ml of aqueous solution containing 10 mg ml⁻¹ PEG-PEDA was pre-incubated with varied volumes of HEX. (B) Interfacial tension of HEX and deionized water under different conditions. In the PEG-PEDA group, PEG-PEDA at 10 mg ml⁻¹ was not pre-incubated with HEX, while 10 μl HEX was pre-incubated with 1 ml of various concentrations of PEG-PEDA in other groups. (C) Digital photos (left) and quantified diameter values (right) showing changes in HEX/PEG-PEDA o/w nanoemulsions after addition of varied volumes of water soluble propionic acid. (D) Digital photos showing nanoemulsification and emulsion breaking upon addition of propionic acid using Nile red-doped HEX. (E) Digital photos (left) and quantified diameter values (right) indicating changes in HEX/PEG-PEDA o/w nanoemulsions after addition of varied EDA. (F) Digital photos illustrating nanoemulsification and emulsion breaking before and after addition of EDA using Nile red-doped HEX. (G) Digital photos showing mixing of HEX with aqueous solution of 10 mg ml⁻¹ PEG-PEDA containing 0.9% NaCl. (H) Digital photos indicating demulsification of HEX/PEG-PEDA nanoemulsions upon addition of 10 mg NaCl. Nanoemulsions were formed by emulsifying 40 μl HEX into 1 ml aqueous solution of PEG-PEDA at 10 mg ml⁻¹. Data are mean ± s.d. ($n = 3$); *** $p < 0.001$.

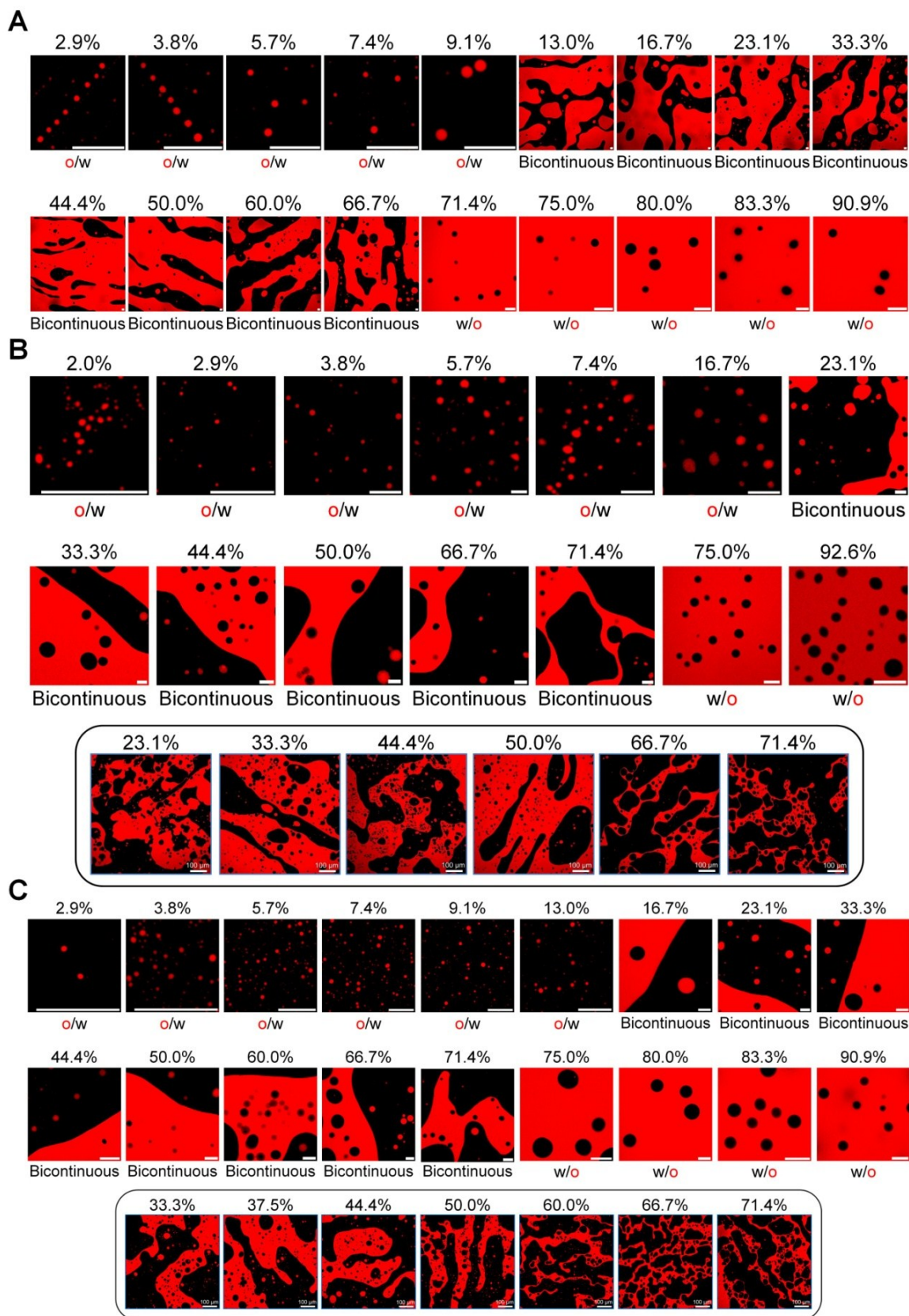


Figure S12. Catastrophic phase inversion of emulsions assembled by HEX/PEG-PEDA. (A-C) Representative fluorescence images indicating phase inversion of emulsions assembled at 10 mg ml⁻¹ (A), 5.0 mg ml⁻¹ (B), and 20.0 mg ml⁻¹ (C) of PEG-PEDA. For emulsions at 5 or 20 mg ml⁻¹ of PEG-PEDA, the corresponding low-magnification views are illustrated for bicontinuous phase. Scale bars represent 10 μ m, except the low resolution images with scale bars of 100 μ m.

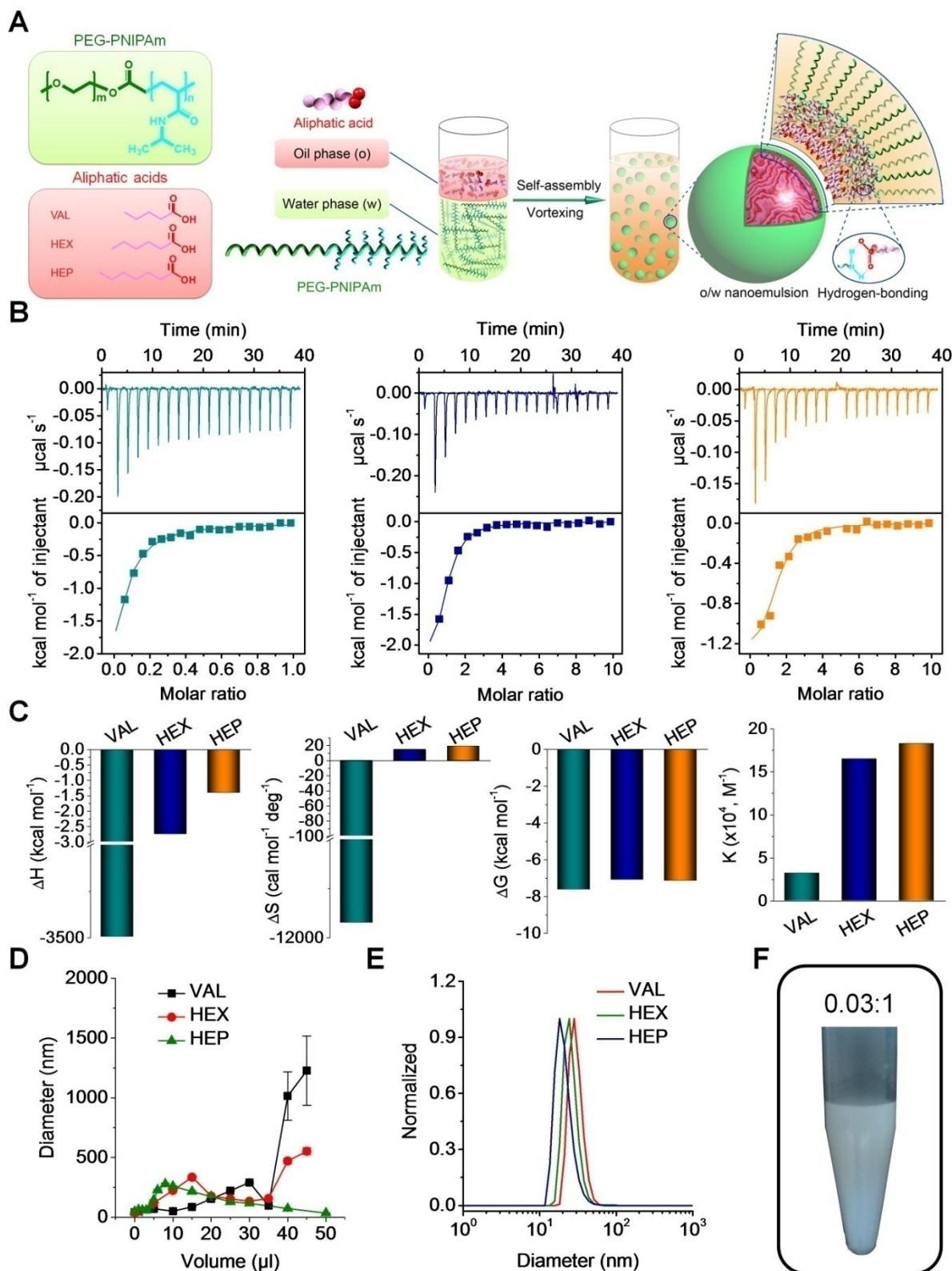


Figure S13. Hydrogen-bonding mediated assembly of emulsions by AAs and aqueous solution of PEG-PNIPAm. (A) Schematic illustration of self-assembly of emulsions mediated by hydrogen-bonding. (B-C) ITC curves (B) and quantified thermodynamic parameters (C) of PEG-PNIPAm and different AAs in aqueous solutions. (D) Changes in the mean diameter of 1 ml of aqueous solution containing 10 mg ml⁻¹ PEG-PNIPAm with increased volumes of different AAs. (E) Size distribution profiles of nanoemulsions at the AA/PNIPAm volume ratio of 0.03:1. (F) A representative digital photo of HEX/PNIPAm nanoemulsions at an oil-water ratio of 0.03:1. Data in (D) are mean \pm s.d. ($n = 3$).

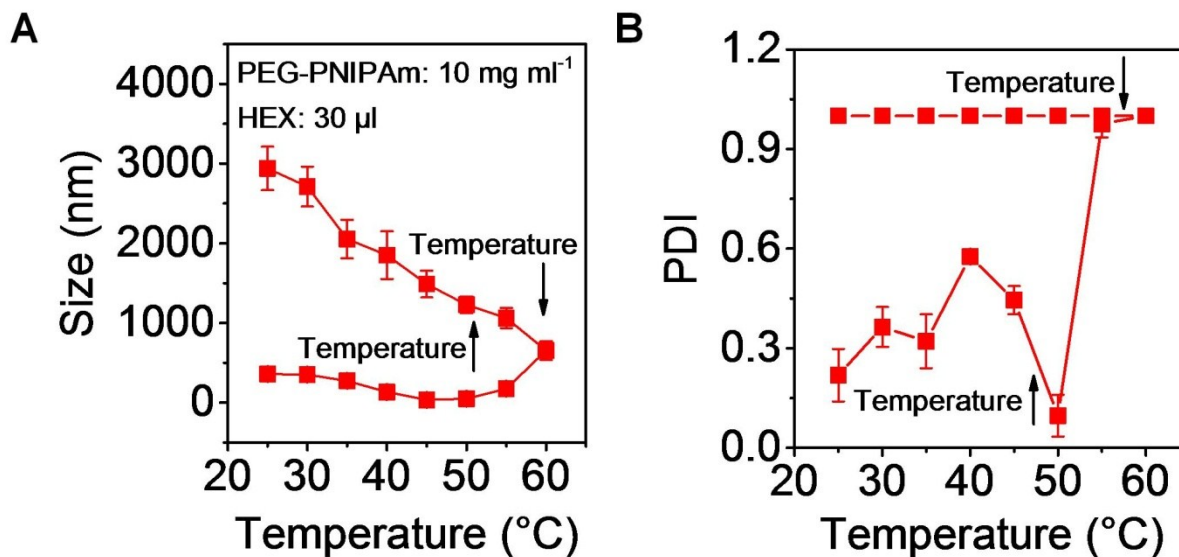


Figure S14. The effect of temperature on HEX/PEG-PNIPAm nanoemulsions. (A-B) Increased temperature-induced changes of the mean diameter (A) and PDI (B) values of assembled nanoemulsions formed by vortexing of 30 μl HEX into 1 ml aqueous solution of PEG-PNIPAm at 10 mg ml^{-1} . Data are mean \pm s.d. ($n = 3$).

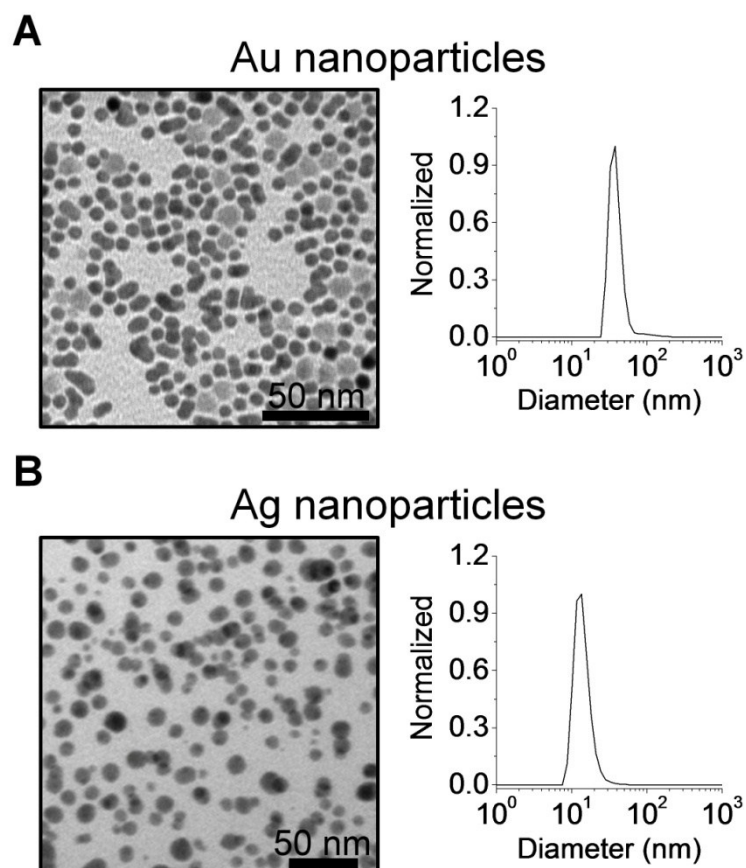


Figure S15. Characterization of Au and Ag nanoparticles. (A-B) TEM images (left) and size distribution profiles (right) of Au (A) or Ag (B) nanoparticles used for solubilization experiments. For TEM sampling or size distribution measurements, powdered Au or Ag nanoparticles were dissolved in chloroform.

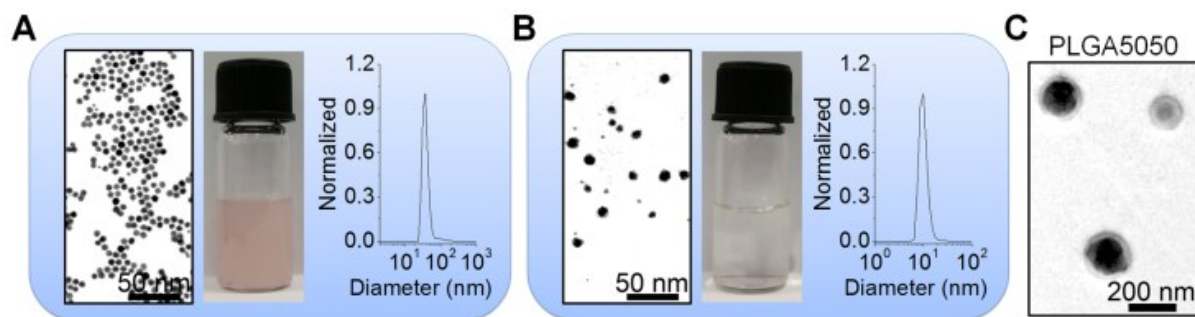


Figure 16. Engineering of nanomaterials via self-assembled emulsions. (A-B) Solubilization of Au (A) or Ag (B) nanoparticles in aqueous solutions by HEX/PEG-PEDA o/w nanoemulsions. The left panels show TEM images of nanoparticles after dispersion in aqueous solutions, while the middle panels are digital photos. The right panels illustrate the size distribution profiles. (C) TEM image of nanoparticles derived from PLGA with a monomer ratio of 50:50 (PLGA5050) fabricated using HEX/PEG-PEDA o/w nanoemulsions.